

Thermodynamic measurement of Nd–Fe system by double Knudsen cell mass spectrometry

Takashi Nagai*, Sho Shirai, Masafumi Maeda

Institute of Industrial Science, The University of Tokyo 4-6-1 Komaba, Meguro-Ku, Tokyo 153-8505, Japan

ARTICLE INFO

Article history:

Received 21 October 2010

Received in revised form

17 December 2010

Accepted 22 December 2010

Available online 12 January 2011

Keywords:

Thermodynamics

Neodymium–iron alloy

Gibbs energy

ABSTRACT

The activities of Nd in the Nd–Fe alloys were determined by double Knudsen cell mass spectrometry. The activities of Nd in Nd–Fe alloys with Nd concentration from 8.5 to 93 at% were determined at 1373–1523 K, measuring the ion current of vapor of Nd in equilibrium with melts, $\text{Nd}_2\text{Fe}_{17} + \gamma\text{Fe}$, $\text{Nd}_2\text{Fe}_{17} + \text{liquid}$, and $\gamma\text{Fe} + \text{liquid}$. The standard Gibbs energy of formation of $\text{Nd}_2\text{Fe}_{17}$ was calculated from the activities of Nd obtained from the measurement, as follows: $2\text{Nd}(\text{l}) + 17\text{Fe}(\gamma) = \text{Nd}_2\text{Fe}_{17}(\text{s})$, $\Delta G_{\text{fNd}_2\text{Fe}_{17}}^\circ = -238,000 + 130T \pm (21,000)\text{J/mol}$ (1373–1473 K).

The activities of Fe in Nd–Fe alloys were calculated based on the Gibbs–Duhem equation.

© 2011 Elsevier B.V. All rights reserved.

1. Introduction

Rare Earth (RE) metals are used as various functional materials, including permanent magnets [1,2], hydrogen storage alloys [3,4] and luminescent materials [5,6]. The consumption of Nd is increasing dramatically because of an exceptionally high demand for Nd–Fe–B–(Dy) magnets and a significant amount of the magnets are wasted [7]. Some researchers have reported on the recycling process for these metals [7–10].

Thermodynamic properties of a system containing RE metal at high temperature are very important to produce and recycle the materials. The properties cannot, however, be measured easily by traditional methods, because the chemical affinities of a RE metal with oxygen are very strong [11]. Therefore, the thermodynamic properties of a Nd–Fe binary system at high temperature are not available and thermodynamic information on intermetallic compounds in these systems is extremely limited.

Double Knudsen mass spectrometry is suitable to investigate the properties. The vapor pressure of the metals in equilibrium with the alloys could be measured by this method if containers of the metals were chosen properly, because the measurement could be run under low oxygen partial pressure with high vacuum condition. The thermodynamic properties of RE metals in alloys can be determined by the vapor pressure, and those in Fe–La and

Fe–Y binary alloys were investigated by this method in previous studies [12,13]. In this study, the thermodynamic properties of a Nd–Fe binary system were measured by double Knudsen mass spectrometry.

2. Experimental

2.1. Preparation of alloys

Fig. 1 shows the phase diagram of Nd–Fe [14]. It has intermetallic compounds, $\text{Nd}_2\text{Fe}_{17}$ and $\text{Nd}_5\text{Fe}_{17}$. Nd–Fe alloys used in this study as specimens were prepared by melting reagent grade Nd grain (99.9%) and electrolytic Fe (99.99%) under high vacuum (ca. 1.0×10^{-3} Pa) with an electron beam melting. The apparatus for electron beam melting was described elsewhere [15]. The maximum power of the electron beam gun is 8 kW, and this gun generates an electron beam with a thermal electron from a tungsten filament. Volume of a vacuum chamber is 0.06 m^3 , and the inside of the chamber is evacuated by a rotary pump ($65\text{ m}^3\text{ h}^{-1}$), a mechanical booster pump ($253\text{ m}^3\text{ h}^{-1}$) and a turbo molecular pump ($3600\text{ m}^3\text{ h}^{-1}$). A water-cooled copper crucible 60 mm in diameter is placed on the bottom of the chamber.

The alloys were melted four or five times, and were reversed up and down or crushed at each run to mix them homogeneously. The chemical compositions of the master alloys were determined by chemical analysis with inductively coupled plasma atomic spectroscopy (ICP–AES, SPS4000, Seiko Instruments Inc.). 8.5, 16, 49, 72, and 93 at%–Nd–Fe alloys were prepared in this study as experimental specimens.

* Corresponding author. Tel.: +81 3 5452 6298; fax: +81 3 5452 6299.
E-mail address: nagai@iis.u-tokyo.ac.jp (T. Nagai).

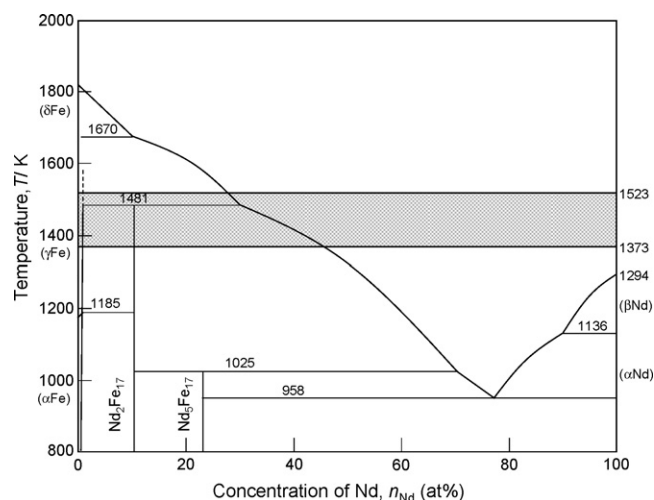


Fig. 1. Phase diagram of Nd–Fe system.

2.2. Double Knudsen cell mass spectrometry

Knudsen cell mass spectrometry was developed as a method to measure vapor pressure of gaseous species in equilibrium with alloys and compounds. In this method, vapor pressure of i -species, P_i , is monitored as ion current, I_i , which is proportional to the pressure [16].

$$P_i = k_i T I_i \quad (1)$$

where T and k_i are the absolute temperature and the constant including device constant and ionization cross section, respectively. Double Knudsen cells allow the measurement of ion currents of evaporated species from two or more substances under identical conditions in an experimental run. Comparing ion currents from an experimental specimen and reference substance, which is typically a pure substance, activity of i -species, a_i , can be deduced directly without the constant, k_i .

$$a_i = \frac{P_{i,\text{specimen}}}{P_{i,\text{reference}}} = \frac{I_{i,\text{specimen}}}{I_{i,\text{reference}}} \quad (2)$$

Details of the equipment used in the double Knudsen cell mass spectrometry are described elsewhere [12,13,17–21]. A cell holder in a vacuum chamber could hold four Knudsen cells. Ion currents from each cell or background could be detected individually by rotating the cell holder. The cells were heated by a Ta electric resistance heating element, and temperatures of those cells were measured by three Pt–13%Rh/Pt thermocouples placed in holes drilled at the bottom of the cell holder.

A quadrupole mass spectrometer (QMS, Leybold Inficon 300 M) was used to monitor and measure ion currents of the evaporated species. The QMS was placed on top of the vacuum chamber in which the Knudsen cell unit was installed. The inside of the chamber was evacuated by a rotary pump and a turbo molecular pump (TMP, 0.5 m³/s), and the vacuum degree was kept below 1.0 × 10^{−4} Pa during experiments. The atomic or molecular beams of evaporated species from the Knudsen cell were injected into the ion source in QMS, where they were converted into positive ions by impact of the electrons emitted from the heated filament. Emission current of the filament and ionization potential were 2000 μA and 102 eV, respectively. The ions in the ion source were injected into the quadrupole mass filter, which rejected all except those of a specific mass-to-charge ratio (m/z); thereafter masses were detected by an electron multiplier.

Reagent grade pure Nd grain (99.9%) was used as a reference for the measurements of Nd–Fe alloys. Since Nd is easily oxidized in

Table 1
Conditions for activity measurement of Nd–Fe alloys.

Exp. #	Temperature, T (K)	Mole fraction of Nd, X_{Nd}	Phase
1		0.085	(Nd ₂ Fe ₁₇ + γFe) – (γFe + liquid)
2		0.16	(Nd ₂ Fe ₁₇ + liquid) – (γFe + liquid)
3	1373–1523	0.49	Liquid
4		0.72	Liquid
5		0.93	Liquid

air, the Nd grains were preserved in spindle oil. Nd–Fe alloys and Nd grains were put into a high vacuum chamber for the measurement as soon as possible after being taken out of the oil and ground with sandpaper, then, rinsed by acetone and ethanol within a few minutes. About 0.2 g of the experimental specimens, which were Nd–Fe alloys, and reference specimen, which was pure Nd, were charged to each Mo Knudsen cell with an Y₂O₃ inner crucible. The cells had a diameter of 10 mm, a height of 20 mm and the thickness of 1 mm. The lid of the cell had an orifice; the diameter of which was 0.4 mm.

According to Knudsen [22], the diameter of the orifice of a Knudsen cell must be less than one tenth of the mean free path of evaporated species so that Knudsen effusion is achieved. Mita et al. [23], by measuring the vapor pressure of zinc, demonstrated that an ion current proportional to partial pressure was detected. The orifice of the Knudsen cell in this study provided an equilibrium condition between gaseous and condensed phases at the experimental temperature. As mentioned, the cell holder could hold four Knudsen cells. In each measurement, experimental alloys were charged to two of them, one reference (pure Nd) was put into a cell and the fourth cell was empty to measure ion current of the background. The experimental conditions (i.e., temperature range, concentration of Nd in Nd–Fe alloy, and measured phase) are summarized in Table 1.

3. Results and discussion

Ion currents from the Nd–Fe alloys and pure Nd were measured by double Knudsen cell mass spectrometry at 1373–1523 K. The ion currents were monitored by scanning mass-to-charge ratio, m/z , and the scan was repeated about 60 times for each specimen. Before and after the measurement of the specimen, background of the ion currents was measured in the same way. Typical results of the ion current during a measurement at 1473 K are shown in Fig. 2. From the Nd–Fe alloys and pure Nd, ion currents were clearly detected at $m/z = 142–146, 148, 150$, which were due to ¹⁴²Nd, ¹⁴³Nd, ¹⁴⁴Nd, ¹⁴⁵Nd, ¹⁴⁶Nd, ¹⁴⁸Nd, and ¹⁵⁰Nd. The differences between the average ion currents from Nd–Fe alloys (experimental specimens) and pure Nd (reference substance) and that of background were taken as the net ion currents of experimental specimens or reference substance. The detected ion currents of Nd from pure Nd at 1473 K are listed in Table 2 with the natural abundance of Nd [24]. The ratio of ion currents was in good agreement with the natural abundance

Table 2
Ion current of Nd from pure Nd at 1473 K.

Mass-to-charge, m/z	Ion current from pure Nd, I_i (A)	Natural abundance of Nd (%)
142	1.03 × 10 ^{−11}	27.1
143	4.39 × 10 ^{−12}	12.2
144	8.72 × 10 ^{−12}	23.8
145	2.72 × 10 ^{−12}	8.3
146	5.97 × 10 ^{−12}	17.2
148	1.93 × 10 ^{−12}	5.8
150	1.84 × 10 ^{−12}	5.6

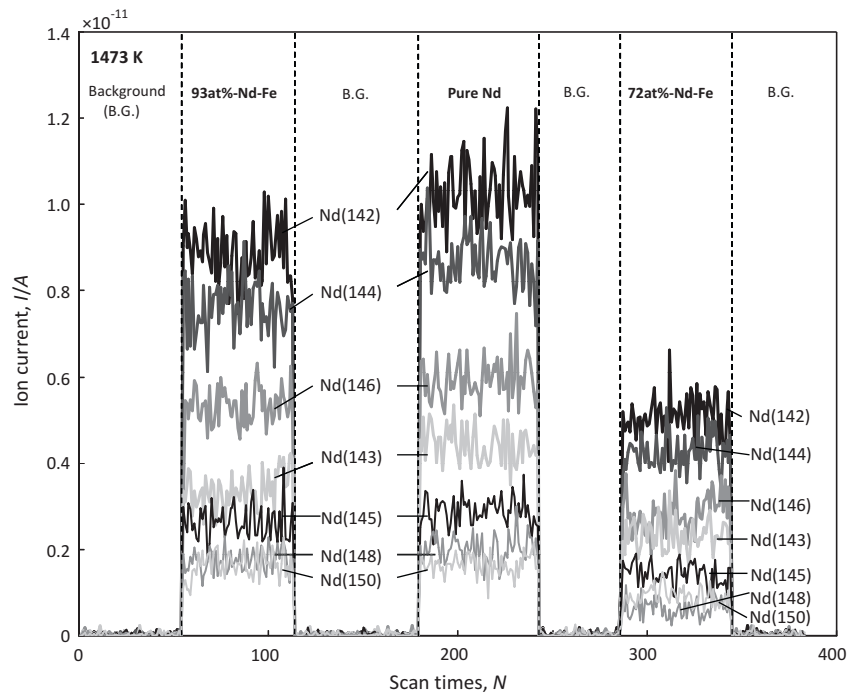


Fig. 2. Ion currents from pure Nd and Nd–Fe alloys.

of Nd. The sum of the ion currents at $m/z = 142–146, 148, 150$ was used as the ion current of Nd in the calculation of the activity.

Meanwhile, ion currents at $m/z = 54, 56, 57$ and 58 , which were due to ^{54}Fe , ^{56}Fe , ^{57}Fe , and ^{58}Fe could not be detected in most experiments, since the vapor pressure in equilibrium with the alloys are too low to be detected.

As indicated by Eq. (2), the activities of Nd in the alloys can be determined as the proportion of ion currents of Nd from Nd–Fe alloys to that from pure Nd. The activities of Nd are listed in Table 3. In the measurements for the 49, 72, and 93 at% Nd–Fe alloys, which exist as Nd–Fe melt at 1373–1523 K, negative deviation is observed and the activities are closer to the ideal solution with rising temperature. Fig. 3 shows the chemical potential, $RT \ln a_{\text{Nd}}$, against temperature calculated with the determined activities of Nd in Nd–Fe alloys with increasing temperature, the value of $RT \ln a_{\text{Nd}}$ in each alloy with 49, 72, and 93 at% Nd slightly increase linearly. The value of 16 at% Nd–Fe alloy decreases with rise in experimental temperature. According to the phase diagram of the Nd–Fe binary system, 16 at% Nd–Fe alloy exists as two phases with $\text{Nd}_2\text{Fe}_{17}$ and Nd–Fe melt under 1481 K, γFe and Nd–Fe melt over the temperature. The composition of the Nd–Fe melt is indicated by the liquidus line. Since the Nd concentration of this line is smaller as the experimental temperature rises, the activity becomes lower. The slope of lines for the alloy with 8.5 at% Nd changed at around 1481 K, because the phase of the alloy changed from solid $\text{Nd}_2\text{Fe}_{17}(\text{s}) + \gamma\text{Fe}$ to $\gamma\text{Fe} + \text{Nd–Fe melt}$ at this temperature. In addition, the value

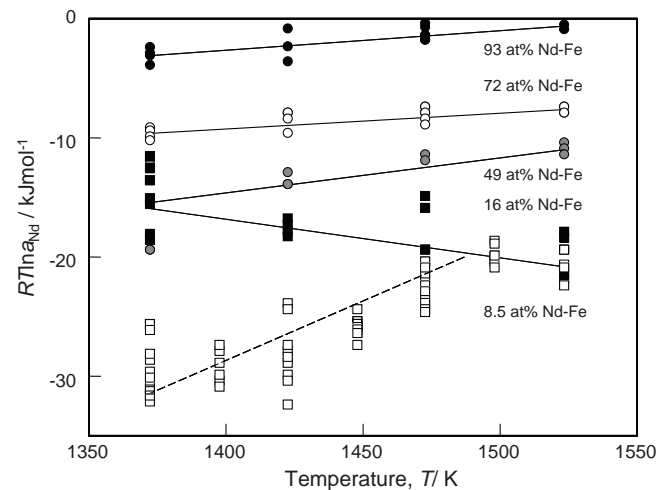


Fig. 3. Chemical potential of Nd in Nd–Fe alloys.

above 1481 K is in good agreement with that of 16 at% Nd–Fe for the Nd content of Nd–Fe melt under these experimental conditions is the same as that described by the liquidus line.

Using the measured activities of Nd in 8.5 at% Nd–Fe alloy, the standard Gibbs energy of formation of $\text{Nd}_2\text{Fe}_{17}$, $\Delta G_{\text{fNd}_2\text{Fe}_{17}}^\circ$, is

Table 3
Activity of Nd in Nd–Fe alloy.

Temperature, T (K)	Activity of Nd, a_{Nd}				
	0.085	0.16	0.49	0.72	0.93
1373	0.079 ± 0.015	0.27 ± 0.06	0.28 ± 0.06	0.43 ± 0.01	0.77 ± 0.03
1398	0.082 ± 0.009				
1423	0.096 ± 0.020	0.23 ± 0.01	0.32 ± 0.01	0.48 ± 0.03	0.84 ± 0.08
1448	0.11 ± 0.01				
1473	0.15 ± 0.02	0.24 ± 0.05	0.39 ± 0.01	0.52 ± 0.02	0.91 ± 0.04
1498	0.21 ± 0.01				
1523	0.19 ± 0.01	0.21 ± 0.03	0.42 ± 0.01	0.55 ± 0.01	0.95 ± 0.01

derived. By the X-ray diffraction pattern of 8.5 at% Nd–Fe alloy, the specimen was identified as a mixture of $\text{Nd}_2\text{Fe}_{17}$ and γFe ; therefore, it is believed that the specimen at the experimental temperature was a mixture of $\text{Nd}_2\text{Fe}_{17}$ and γFe . The equilibrium reaction in this alloy can be expressed by Eq. (3), and there is a relationship among the chemical potentials of component i , μ_i 's, since the chemical potentials on both sides should be equal when these phases are in equilibrium.



$$\mu_{\text{Nd}_2\text{Fe}_{17}} = 2\mu_{\text{Nd}} + 17\mu_{\text{Fe}} \quad (4)$$

Eq. (4) can be written with μ_i° 's and activities of i as follows.

$$\mu_{\text{Nd}_2\text{Fe}_{17}}^\circ + RT \ln a_{\text{Nd}_2\text{Fe}_{17}} = 2(\mu_{\text{Nd}}^\circ + RT \ln a_{\text{Nd}}) + 17(\mu_{\text{Fe}}^\circ + RT \ln a_{\text{Fe}}) \quad (5)$$

The activity of $\text{Nd}_2\text{Fe}_{17}$ is equal to unity since the compound is stoichiometric. The activities of Fe are also equal to unity since solubility of Nd to Fe is insignificant.

$$\mu_{\text{Nd}_2\text{Fe}_{17}}^\circ - 2\mu_{\text{Nd}}^\circ - 17\mu_{\text{Fe}}^\circ = 2RT \ln a_{\text{Nd}} \quad (6)$$

The following equations were, thus, eventually derived.

$$\Delta G_{\text{fNd}_2\text{Fe}_{17}}^\circ = 2RT \ln a_{\text{Nd}} \quad (7)$$

Using the measured values a_{Nd} , $\Delta G_{\text{fNd}_2\text{Fe}_{17}}^\circ$ could be determined to be

$$\Delta G_{\text{fNd}_2\text{Fe}_{17}}^\circ = -238,000 + 130T \pm (21,000) \text{ J/mol} \quad (1373\text{--}1473 \text{ K}) \quad (8)$$

The assigned uncertainty was estimated by the standard deviation of the value based on Eq. (7).

Hennemann et al. [25] reported the Gibbs energy change of the following reaction.



$$\Delta G_{\text{fNd}_2\text{Fe}_{17}}^\circ = -34,380 - 12T \pm (40) \text{ J/mol} \quad (298\text{--}1184 \text{ K}) \quad (10)$$

Takeda et al. [8] calculated the Gibbs energy of formation of $\text{Nd}_2\text{Fe}_{17}$ as Eq. (15) by extrapolating the value of this equation and using thermodynamic data of the phase transformation of Nd and Fe (Eqs. (11)–(14)).



$$\Delta G_{\text{transNd}}^\circ = 64140 + 77.72T \log T - 292T \text{ J/mol} \quad (1294\text{--}3400 \text{ K}) \quad (12)$$



$$\Delta G_{\text{transFe}}^\circ = 53,050 + 77.93T \log T - 284.5T \text{ J/mol} \quad (1185\text{--}1667 \text{ K}) \quad (14)$$

$$\Delta G_{\text{fNd}_2\text{Fe}_{17}}^\circ = -1,064,000 - 1480T \log T + 5408T \text{ J/mol} \quad (1294\text{--}1667 \text{ K}) \quad (15)$$

This can be expressed as Eq. (16) in the temperature range of 1294–1481 K:

$$\Delta G_{\text{fNd}_2\text{Fe}_{17}}^\circ = -175,000 + 115T \text{ J/mol} \quad (1294\text{--}1481 \text{ K}) \quad (16)$$

The Gibbs energy of formation of $\text{Nd}_2\text{Fe}_{17}$ determined in this study is shown in Fig. 4 with that by a previous study [25]. This value is ca. 40 kJ higher than that determined at 1373–1473 K in present study although the slope of the two equations is similar.

The activities at 1373 K were re-plotted against the composition of the alloy in Fig. 5. The open circles in the figure indicate the activities of Nd. Since the activities of Nd were measured over a wide range of composition, it is also possible to derive the activities of Fe based on the Gibbs–Duhem equation. Fe activities were calculated from the Nd activities using following Eq. (17):

$$\ln \gamma_{\text{Fe}} = - \int_{\ln \gamma_{\text{Nd}}^\circ}^{\ln \gamma_{\text{Nd}}} \frac{X_{\text{Nd}}}{X_{\text{Fe}}} d \ln \gamma_{\text{Nd}} \quad (17)$$

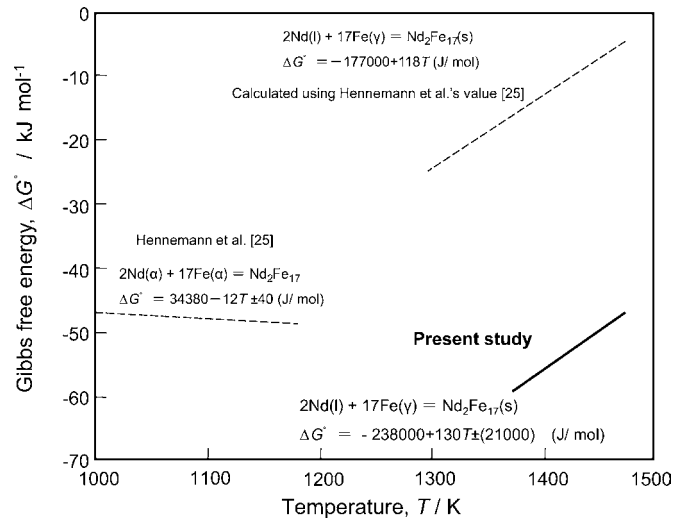


Fig. 4. Standard Gibbs energy for formation of $\text{Nd}_2\text{Fe}_{17}$.

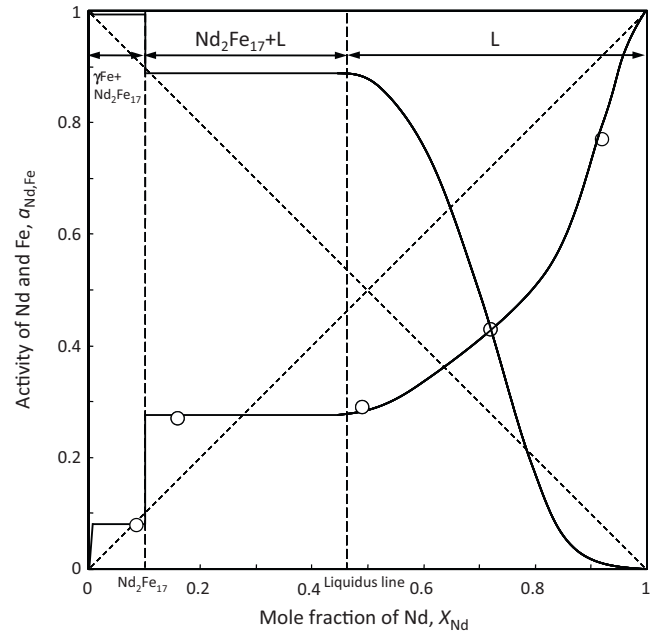


Fig. 5. Composition dependence of activities of Nd and Fe in Nd–Fe alloys at 1373 K.

where γ_i and X_i are activity coefficient and mole fraction of i component, respectively. Using the activity coefficient on the liquidus line, γ_i^{L} , the following equation was obtained:

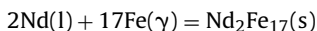
$$\ln \gamma_{\text{Fe}} = \ln \gamma_{\text{Fe}}^{\text{L}} - \int_{\ln \gamma_{\text{Nd}}^{\text{L}}}^{\ln \gamma_{\text{Nd}}} \frac{X_{\text{Nd}}}{X_{\text{Fe}}} d \ln \gamma_{\text{Nd}} \quad (18)$$

The composition of liquidus line is based on the phase diagram, and activity of Fe in the two phase region, $\text{Nd}_2\text{Fe}_{17} + \text{Nd–Fe}$ melt, which is equal to that on the liquidus line, was calculated by the activity of Nd in 16 at% Nd–Fe alloy and the standard Gibbs energy of formation of $\text{Nd}_2\text{Fe}_{17}$ (Eq. (8)). The derived Fe activities at 1373 K are also shown in Fig. 5.

4. Conclusions

The activities of Nd in Nd–Fe alloys with Nd concentration from 8.5 to 93 at% were determined at 1373–1523 K, measuring the ion current of the vapor of Nd in equilibrium with Nd–Fe

melts, $\text{Nd}_2\text{Fe}_{17} + \gamma\text{Fe}$, $\text{Nd}_2\text{Fe}_{17} + \text{liquid}$, and $\gamma\text{Fe} + \text{liquid}$. The standard Gibbs energy of formation of $\text{Nd}_2\text{Fe}_{17}$ was calculated from the activities of Nd obtained from the measurement as follows:



$$\Delta G_{f, \text{Nd}_2\text{Fe}_{17}}^\circ = -238,000 + 130T \pm (21,000) \text{ J/mol} \quad (1373\text{--}1473 \text{ K})$$

The activities of Fe in Nd–Fe alloys were determined based on the Gibbs–Duhem equation.

Acknowledgments

The authors thank Professor Kazuki Morita in Institute of Industrial Science, The University of Tokyo for helpful discussion and advice throughout this project.

References

- [1] J.J. Croat, J.F. Herbst, R.W. Lee, F.E. Pinkerton, Pr–Fe and Nd–Fe-based materials—a new class of high-performance permanent-magnets, *J. Appl. Phys.* 55 (1984) 2078–2082.
- [2] M. Sagawa, Developments in Nd–Fe–B permanent magnets, *Mater. Jpn.* 40 (2001) 943–946.
- [3] K.H.J. Buschow, in: K.A. Gschneidner Jr., L. Eyring (Eds.), *Handbook on the Physics and Chemistry of Rare Earths*, vol. 6, Elsevier, Amsterdam, 1984.
- [4] N. Sato, N. Morishita, T. Kimura, N. Fujioka, O. Takahishi, S. Bito, Y. Hattori, Y. Dansui, M. Ikoma, Nickel-metal hydride battery for hybrid electric vehicles, *Matsushita Tech. J.* 48 (2002) 15–20.
- [5] J.E. Geusic, H.M. Marcos, L.G. Van Uitert, Laser oscillations in Nd-doped yttrium aluminum yttrium gallium + gadolinium garnets (continuous operation of $\text{Y}_3\text{Al}_5\text{O}_{12}$ pulsed operation of $\text{Y}_3\text{Ga}_5\text{O}_{15} + \text{Gd}_3\text{Ga}_5\text{O}_{12}$ room temperature), *Appl. Phys. Lett.* E 4 (1964) 182–184.
- [6] K. Ohno, T. Abe, Bright green phosphor $\text{Y}_3\text{Al}_5\text{--XGa}_5\text{O}_{12}\text{--Tb}$, for projection CRT, *J. Electrochem. Soc.* 134 (1987) 2072–2076.
- [7] O. Takeda, T.H. Okabe, Y. Umetsu, Recovery of neodymium from a mixture of magnet scrap and other scrap, *J. Alloys Compd.* 408–412 (2006) 387–390.
- [8] O. Takeda, T.H. Okabe, Y. Umetsu, Phase equilibrium of the system Ag–Fe–Nd, and Nd extraction from magnet scraps using molten silver, *J. Alloys Compd.* 374 (2004) 305–313.
- [9] O. Takeda, T.H. Okabe, Y. Umetsu, Phase equilibria of the system Fe–Mg–Nd at 1076 K, *J. Alloys Compd.* 392 (2005) 206–213.
- [10] T.H. Okabe, O. Takeda, K. Fukuda, Y. Umetsu, Direct extraction and recovery of neodymium metal from magnet scrap, *Mater. Trans.* 44 (2003) 798–801.
- [11] I. Barin, *Thermochemical Data of Pure Substance*, VCH Verlagsgesellschaft mbH, Weinheim, 1989.
- [12] W.H. Han, T. Nagai, M. Miyake, M. Maeda, *Metall. Mater. Trans. B* 40B (2009) 656–661.
- [13] T. Nagai, W.H. Han, M. Maeda, Thermodynamic measurement of La–Fe and Y–Fe alloy by multi Knudsen cell mass spectrometry, *J. Alloys Compd.* 507 (2010) 72–76.
- [14] T.B. Massalski, *Binary Alloy Phase Diagrams*, ASM, Metal Park, OH, 1986.
- [15] T. Ikeda, M. Maeda, Purification of metallurgical silicon for solar-grade silicon by electron-beam button melting, *ISIJ Int.* 32 (1992) 635–642.
- [16] M. Heyrman, C. Chatillon, H. Collas, J. Chemin, Improvements and new capabilities for the multiple Knudsen cell device used in high-temperature mass spectrometry, *Rapid Commun. Mass Sp.* 18 (2004) 163–174.
- [17] T. Nagai, M. Miyake, Y. Mitsuda, H. Kimura, M. Maeda, Mass spectrometric study on phosphorus in molten carbon-saturated iron, *ISIJ Int.* 47 (2007) 207–210.
- [18] T. Nagai, M. Miyake, H. Kimura, M. Maeda, Determination of Gibbs energy of formation of Cr_3P by double Knudsen cell mass spectrometry, *J. Chem. Thermodyn.* 40 (2008) 471–475.
- [19] T. Nagai, Y. Ogasawara, M. Maeda, Thermodynamic measurement of $\text{Al}_2\text{O}_3\text{--B}_2\text{O}_3$ system by double Knudsen cell mass spectrometry, *J. Chem. Thermodyn.* 41 (2009) 1292–1296.
- [20] T. Nagai, M. Miyake, M. Maeda, Thermodynamic measurement of calcium phosphates by double Knudsen cell mass spectrometry, *Metall. Mater. Trans. B* 40 (2009) 544–549.
- [21] W.H. Han, M. Miyake, T. Nagai, M. Maeda, Measurements of vapor pressure of Y and activity of Y in Y–O alloy by multi Knudsen cell mass spectrometry, *J. Alloys Compd.* 481 (2009) 241–245.
- [22] M. Knudsen, The molecular current of gases through openings and the effusion, *Annal. Phys.* 29 (1909) 999–1016.
- [23] K. Mita, S. Yamaguchi, M. Maeda, Vapor pressure measurement of Zn–Fe intermetallic compounds, *Metall. Mater. Trans. B* 35 (2004) 487–492.
- [24] M. Zhao, T. Zhou, J. Wang, H. Lu, F. Xiang, Absolute measurements of neodymium isotopic abundances and atomic weight by MC-ICPMS, *Int. J. Mass Spectrom.* 245 (2005) 36–40.
- [25] K. Henneman, H.L. Lukas, H.J. Schaller, Constitution and thermodynamics of Fe–Nd alloys, *Z. Metall.* 84 (1993) 668–674.